2023

Collagen V Promotes Fibroblast Contractility, And Adhesion Formation, And Stability

Shaina P. Royer-Weeden
Michigan Technological University, sproyer@mtu.edu

COLLAGEN V PROMOTES FIBROBLAST CONTRACTILITY, AND ADHESION FORMATION, AND STABILITY

By

Shaina P. Royer-Weeden

A THESIS

Submitted in partial fulfillment of the requirements for the degree of

MASTER OF SCIENCE

In Biomedical Engineering

MICHIGAN TECHNOLOGICAL UNIVERSITY

2023

This thesis has been approved in partial fulfillment of the requirements for the Degree of MASTER OF SCIENCE in Biomedical Engineering.

Department of Biomedical Engineering

Thesis Advisor:	*Dr. Sangyoon Han*
Committee Member:	*Dr. Jeremy Goldman*
Committee Member:	*Dr. Muhammad Rizwan*
Department Chair:	*Dr. Sean Kirkpatrick*

Table of Contents

Author Contribution Statement

Nikhil Mittal and Mohanish Chandurkar assisted with live cell imaging. Sara Goheen did much of the work with rheology. Nikhil Mittal, Mohanish Chandurkar, and Dr. Sangyoon helped with data analysis. Dr. Sangyoon Han and Scott Severance helped with figure drawing.

Acknowledgements

I would first like to thank the Wallace Research Foundation for providing funding. I would like to thank my advisor Dr. Sangyoon Han for letting me join the lab when I was interested in undergraduate research as a freshman and for being so supportive of me over all these years.

I would like to thank the ACMAL for access to the scanning electron microscope.

Thank you to my parents for the emotional and financial support they have provided over the years. I would like to thank my husband for keeping my life and this paper's grammar together.

I am grateful for coffee for providing me with the motivation to work. Last of all I would like to thank my cat Maverick for her emotional support and all-important contribution of "Meow."

Abstract

Ehlers-Danlos syndrome, classical type, (cEDS) is a hereditary connective tissue disorder causing excessive elasticity and fragility of the connective tissue and problems with wound healing. Most cases of cEDS are caused by haploinsufficiency for collagen V. Collagen V regulates collagen fibril diameter. In cEDS fibroblast migration is impaired and integrin expression is altered.

The effects of collagen V on collagen gel ultrastructure and how it alters its mechanical properties were measured using scanning electron microscopy (SEM) and rheology respectively. Fibroblast contractility and adhesion dynamics were investigated to better understand the role of fibroblast disfunction in wound healing in cEDS. To quantify these, traction force microscopy (TFM) and time lapse imaging were used.

Collagen V decreased fibril diameter and curvature, and increased gel stiffness, indicating that the fibrils themselves were likely stiffer. Cells cultured on collagen V were more contractile and adhesions assembled faster. This indicates that a lack of collagen V may induce fibroblast disfunction that causes the poor wound healing seen in cEDS.

1 Introduction

Ehlers-Danlos Syndromes (EDS) are a group of 13 different hereditary connective tissues disorders that cause laxity, and or fragility in connective tissues [3]. All types of EDS cause ultrastructural abnormalities in the extracellular matrix (ECM) [4-17]. While the genetics of all types except one are well understood, how the mutations lead to the observed phenotype is unclear. All identified genetic mutations in EDS are either in genes for collagen or genes that encode proteins involved in the posttranslational modification of collagen [18]. Because all types of EDS cause changes in the ECM ultrastructure it was initially assumed that the changes in the ECM ultrastructure cause the observed symptoms of EDS [19]. However, a lack of correlation between symptom severity in patients and the degree of abnormality in ultrastructure has cast doubt on such a simplistic explanation [11, 20, 21]. Mechaniobiological factors may provide a better explanation for the observed symptoms in EDS. Despite differences in the kinds of defects in collagen there is similar fibroblast dysfunction found in classical (cEDS), hypermobile (hEDS), and vascular (vEDS). This points to a unifying factor such as connective tissue stiffness [22, 23].

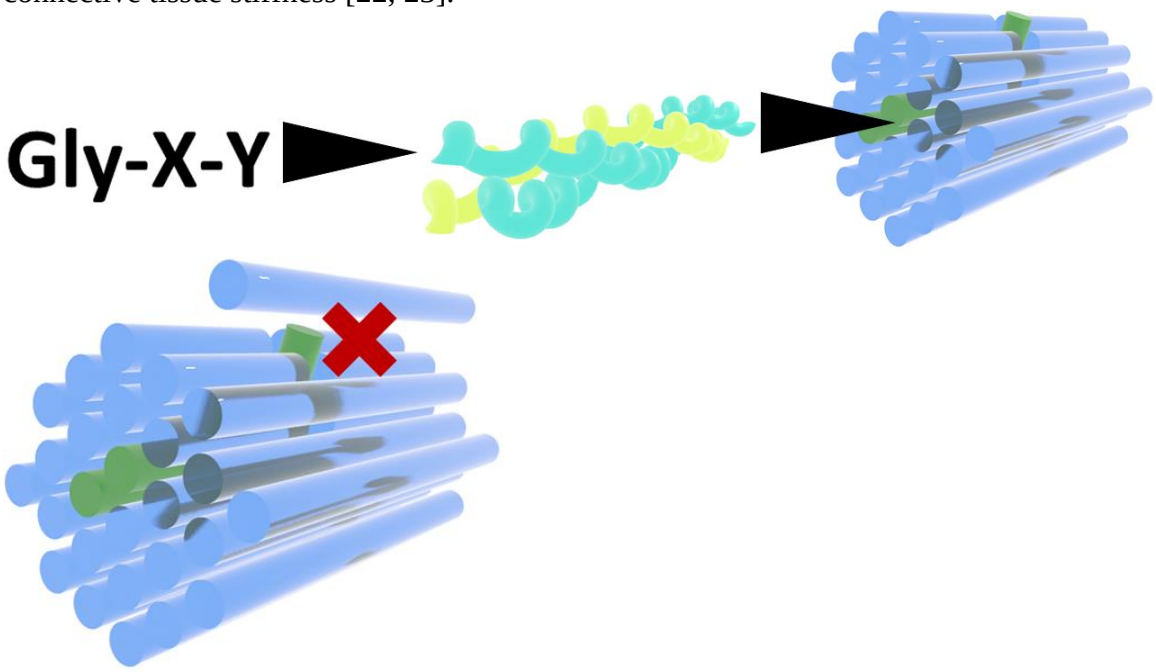

Figure 1.1 Fibrillar types of collagen such as types I and V mainly have a repeating sequence of glycine-X-Y with proline and hydroxyproline being the most common amino acids for X and Y. 3 subunits the main structure of each is a left handed alpha helix assemble to form a collagen protein with a right-handed helix [24]. Collagen proteins pack together to form a fibril. Collagen V shown in green has a kinked N-terminal domain. This is thought to sterically hinder the assembly of collagen fibrils [25].

Classical type EDS (cEDS) is the second most common type of EDS with an approximate incidence of 1:20,000 to 1:40,000 [26]. cEDS causes fragile elastic skin with poor wound healing and atrophic scarring. It also causes joint hypermobility and dislocations. Connective tissue stiffness in cEDS is reduced [27]. However, it is important to note that even within a given type of EDS, presentation is quite variable. In cEDS some collagen fibrils have a large and irregular cross section. Most cases of cEDS are caused by mutations in COL5A1 and result in haploinsufficiency for collagen V. Other rarer causes include mutations in COL5A2 resulting in an abnormal α2 chain for collagen V and COL1A1 p.(Arg312Cys) [1, 28].

Collagen V is a minor type of fibrillar collagen. It has a globular N-terminal domain that sterically hinders the assembly of collagen fibrils, decreasing their diameter. Collagen V is generally found in low concentrations alongside collagen I.

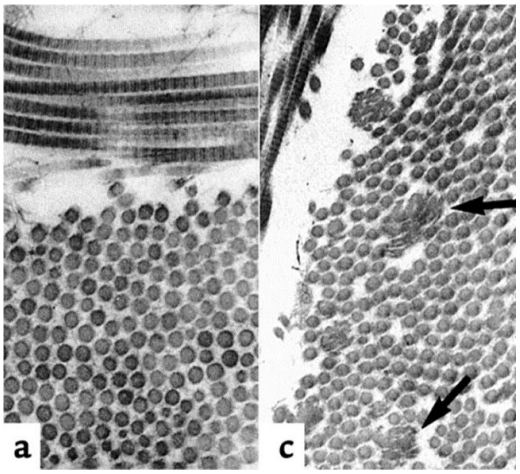

Figure 1.2 Skin biopsy imaged using transmission electron microscopy (TEM). The banded lines in the top of the images are collagen fibrils parallel to their long axis and the dots in the bottom of the images are collagen fibrils perpendicular to their long axis so their cross section can be easily seen. A) In normal skin collagen fibrils have a regular diameter and circular cross section. C) In cEDS some collagen fibrils have a large and irregular cross section [29].

cEDS can be in many ways thought of as the opposite of fibrotic disease. In cEDS tissue stiffness is reduced and wounds heal with atrophic scarring. In fibrotic disease tissue stiffness is increased, with excessive production of connective tissue causing hypertrophic scarring. Likewise, in contrast to fibrotic disease, tissue stiffness and collagen production is reduced in cEDS. cEDS and fibrosis, which have both opposite symptoms and opposite forms of dysregulation of collagen V, highlight the critical role that collagen V plays in normal function of the extracellular matrix (ECM). However, the mechanics of how collagen V regulates tissue stiffness have yet to be studied [25].

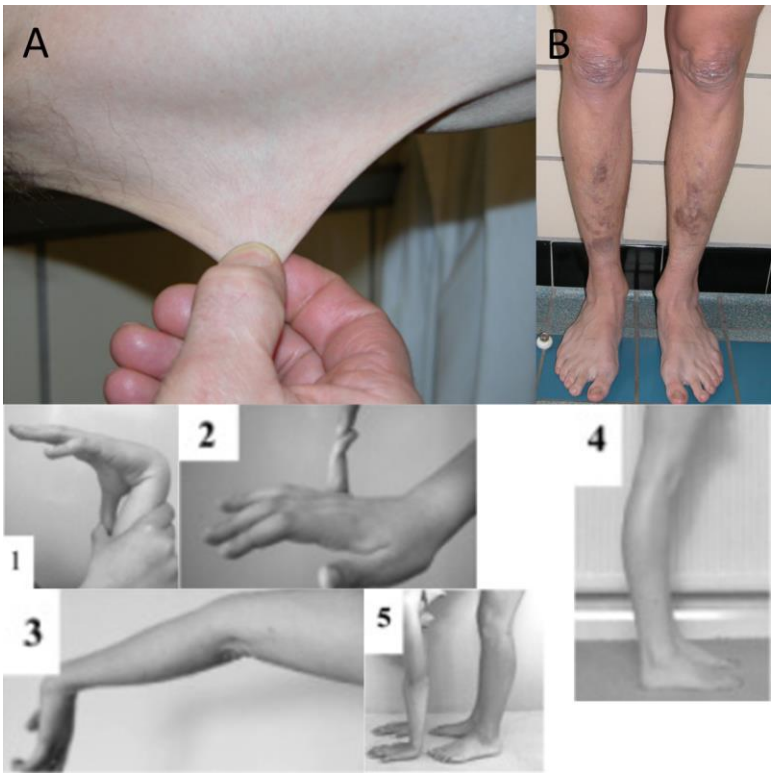

Figure 1.3 Major criteria for cEDS are skin hyperextensibility A) widened atrophic scarring B) and joint hypermobility 1-5) [1]. Hypermobility as demonstrated by the Beighton score. 1-4 are worth 1 point each per side and 5 is worth one point. 1) thumb to forearm 2) pinky expended > 90° 3) elbow hyperextension > 10° 4) knee hyperextension > 10° 5) palms on floor while knees are straight [2, 3].

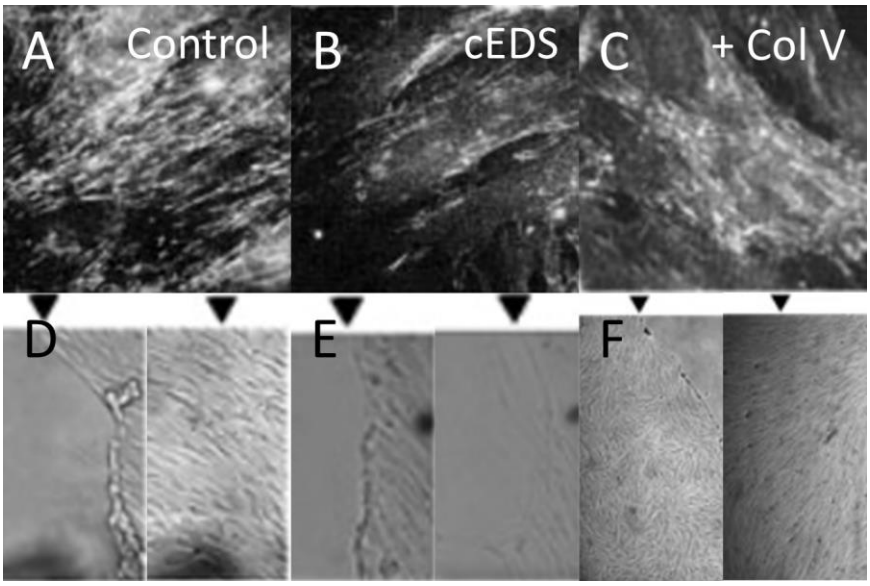

Figure 1.4 A-C) $\alpha_5\beta_1$ expression D-F) Fibroblast migration over 48 hours. A, D) Control fibroblasts with normal $\alpha_5\beta_1$ expression and migration. B, E) cEDS fibroblasts with lowered $\alpha_5\beta_1$ and impaired migration. C, F) Restoration of cEDS fibroblasts to normal with the addition of collagen V [22, 30].

Fibroblasts cultured on a gel containing collagen I and collagen V contract the gel more quickly than those cultured in a gel solely containing collagen I. This suggests that fibroblasts may be more contractile on collagen V [31]. However, that experimental design has a weakness. The effects of cell contractility and gel stiffness in determining the rate of gel contraction cannot be separated from one another. Further experiments where the bulk stiffness is controlled are needed to confirm this finding. Why this would be is unclear; there are no integrins specific to collagen V but not collagen I [32].

In cEDS fibroblasts migration is impaired. This impaired migration may play a role in the impaired wound healing observed in cEDS. Integrin expression of $\alpha_2\beta_1$ and $\alpha_5\beta_1$ is decreased and $\alpha_V\beta_3$ expression is increased. Integrin expression and migration can be restored to normal by adding collagen V to the media [22, 30].

2 Research Aims

cEDS is characterized by a reduction in collagen V. By varying the concentrations of collagen V in coatings and gels, an in vitro model of cEDS can be developed. This model can be used to examine how cEDS affects fibroblasts and the mechanical properties of the ECM.

- Determine the role of collagen V in fibroblast contractility adhesion dynamics.
    - Traction force microscopy was used to quantify contractility on collagen types I and V.
    - Time lapse imaging was used to quantify adhesion dynamics on collagen types I and V.
- Determine the nanoscale morphology and mechanics of collagen V to see if it could be a driver of the mechanotransduction response.
    - Scanning electron microcopy was used to quantify the ultrastructure of collagen gels containing various ratios of collagen types I and V.
    - Rheology was used to quantify the bulk mechanical properties of collagen gels containing various ratios of collagen types I and V.

3 Experiment Methods

3.1 Scanning Electron Microscopy

Collagen gel samples containing 100% collagen I, 10% collagen V, and 20% collagen were prepared with a final collagen concentration of 1.5 mg/mL. Atelo collagen I was used to match the collagen V which was presumably also atelo based on the method of manufacture [33, 34]. Concentrations of collagen V higher than 20% were not used due to the low concentration of collagen V stock solution. Total gel volume was 100 µL. The requisite amounts of collagen V were added to collagen I along with 10 µL 10x phosphate buffered saline (PBS). DI water was added in the collagen I and 10% collagen V conditions to bring the volume up to 70 uL before mixing. 1M and 0.1M NaOH were used to adjust the pH to between 7.2 and 7.6. If needed more DI water was added to bring the total volume to 100 µL. The gels were incubated at 37 °C for 90 minutes. They were then fixed in 1% glutaraldehyde in 0.1M phosphate buffer for 4 hours.

After fixation they were rinsed thrice for 5 minutes in DI water. They were then progressively dehydrated by being submersed for 10 minutes in 25%, 50%, 75%, 90%, and 2 times in 100% ethanol. Following dehydration, the gels were rinsed twice for 10 minutes in hexamethyldisilazane (HMDS) then placed on a glass coverslip and submersed in HMDS which was allowed to evaporate overnight.

The dried gels were then sputter coated with Pt/Pd. The settings used were 5nm and 20ma. HV settings for SEM were 5 kV and 10 µA. 10 images were taken per gel sample at 20,000x magnification. The 8 best images per condition were used for further analysis.

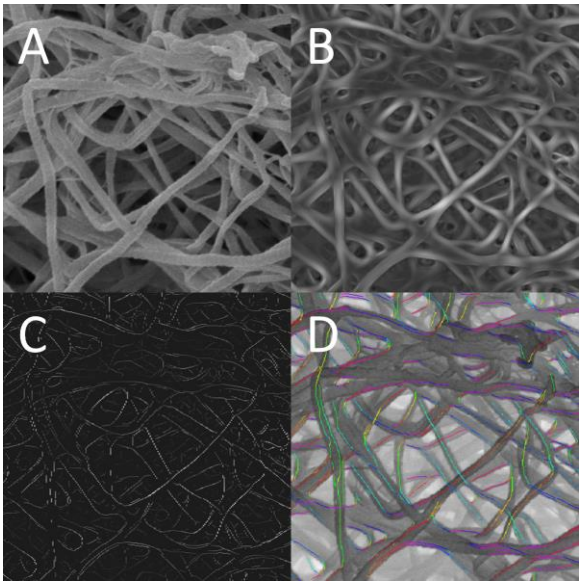

Figure 3.1 A) Raw image B) Steerable filter C) Non maximal suppression D) Segmented fibrils with angle shown by color.

The diameter of the collagen fibrils was measured manually in Image J. Starting from a corner of the image the diameter of every clearly visible fibril was measured until 50 fibrils were measured. If the fibril diameter was variable, the diameter was taken at approximately the middle point.

For measuring curvature, a steerable filter was applied to the images followed by nonmaximal suppression and segmentation.

3.2 Rheology

Collagen gels with 100% collagen I, 10% collagen V, and 20% Collagen V were made as for scanning electron microscopy (SEM). 150 uL of the gel was dispensed onto the cone plate rheometer. The height was set to 0.142 mm and the temperature to 37 °C. The gel was left to cure for 90 minutes. The rheology was done in time sweep mode with 1% strain and 1Hz frequency for 2 hours.

3.3 TFM and Adhesion

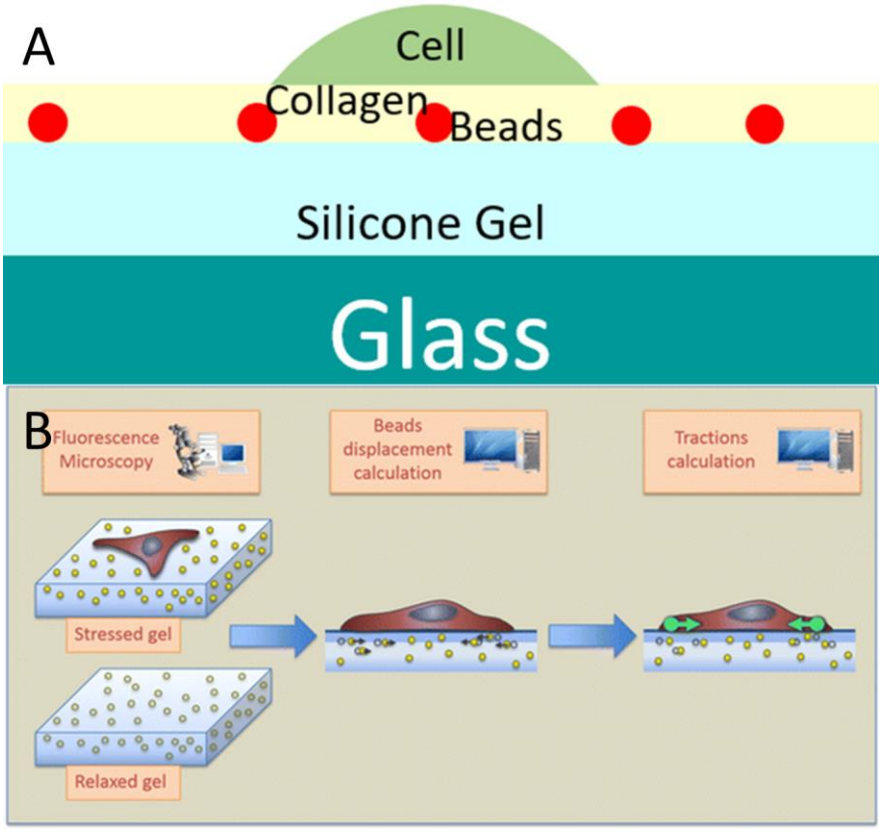

Figure 3.2 A) Cross section of TFM substrate. Silicone gel is coated on a glass bottom dish. Fluorescent beads and either collagen I or collagen V are coated on top of the silicone gel. The collagen layer is very thin, so the deformation mainly takes place in the silicone gel. B) Cells on the TFM substrate contract deforming the substrate. The substrate is imaged both in its deformed state, with the cells on it, and in its relaxed state,

once the cells have been lysed. The displacement of the beads is tracked and from that a traction map is calculated [35, 36].

NIH 3T3 fibroblasts that had been genetically modified to express mRuby-Paxillin were used for all cell culture experiments.

To quantify contractility traction force microscopy (TFM) was used. TFM works by culturing cells of a soft substrate. To track deformation of the substrate fluorescent beads were chemically bonded to the substrate. The gel was first imaged while the cells were alive. The contractile force of living cells deforms the substrate. The cells were then lysed with bleach. When the cells detached the substrate returned to its relaxed position and was imaged again. From there the displacement of the beads was tracked and a traction map was calculated.

The substrate for TFM was fabricated by first spin coating with silicone gel. Q-gel 920 was measured out in a 1:1.2 ratio of parts A:B. It was vortexed to medium high for 2 minutes then mixed by hand for 10 minutes. 110 µL of gel was pipetted into a glass bottom dish. It was spin coated at 250 rpm for 12 seconds with an acceleration of 100 rpm, then at 1000 rpm for 30 seconds with an acceleration of 500 rpm. The gel was cured in a convection oven at 80 °C for 2 hours. The thickness of the gel was approximately 45 µm and stiffness was 2.61kPa. The gels were stored for up to a week in PBS.

The gel was silanized so the beads and collagen could be chemically bonded to it. To silanize it the gel was submersed in 5% 3-aminopropyl triethoxysilane (APTES) for 3 minutes. It was then rinsed thrice with 96% ethanol. The gel was left to air dry.

For bead coating 5 µL of 100 mg/mL N-(3-Dimethylaminopropyl)-N′-ethylcarbodiimide hydrochloride (EDC) and 1 µL of FluoSpheres™ Carboxylate-Modified Microspheres, 0.04 µm, dark red beads were added to 5mL of DI water. It was sonicated for 15 minutes then, as quickly as possible, poured onto the substrate and incubated for 10 minutes at room temperature. It was then rinsed thrice with PBS and kept slightly wet with PBS. The lid and outside of the glass bottom dish were wiped down with 70% ethanol and sterilized with UV light in the biosafety cabinet for 25 minutes.

For collagen coating either collagen I or V were added to 3.1 mL of PBS at a concentration of 1 µL/mL. Collagen I was telocollagen unless noted otherwise. 3.1 µL of 100 mg/mL EDC was added. The solution was briefly vortexed, poured onto the substrate, and incubated for 30 minutes at room temperature. The substrate was then rinsed thrice with PBS.

For TFM and adhesion experiments the cells were seeded at approximately 20% confluency. For the preliminary TFM experiment the cells were imaged 4 hours after seeding. For the later TFM experiment the cells were imaged 5 hours after seeding. For the adhesion dynamics experiments cells were imaged every 15 seconds for 15 minutes 1.5 hours after seeding.

The cells and beads were imaged using total internal reflection (TIRF) microscopy. TIRF works by having your item of interest, in this case a cell and fluorescent beads, on top of an item with a higher index of refraction. Then, by shining a laser at the correct angle on to the item of interest, the image will be reflected back down through the objective. The refractive index of the silicone gel used was 1.49 which is higher than that of the cells which is 1.36 enabling TIRF to be used [37, 38].

The beads and adhesions were illuminated with lasers at 642 and 587 nm respectively. The laser angle was adjusted on the cell channel. The illumination intensity was adjusted to the minimum necessary for a clear image. The exposure time was 300 ms.

The images were analyzed in Matlab using a program developed by Dr. Han. First, a mask to identify the location of the cells was applied. This was done by using the Otsu method of segmentation and then refining the mask by excluding segmented areas smaller than 10 pixels, connecting segmented areas within 3 pixels of each other, excluding that which was not part of the larger object, and filling holes in the larger object.

The locations of the beads were analyzed in both the images with the live cells and the references images. Stage drift was then corrected for and the displacement field was calculated. Outliers were removed from the displacement field. Then, from the displacement field, the gel thickness, and stiffness, a traction map was created. To create the traction map, the inverse problem was solved to go from a displacement field to a stress field. The inverse problem was solved using the Fourier Transform Traction Cytometry (FTTC) method [39].

For adhesion dynamics analysis, subpixel registration was performed on the cell channel followed by thresholding using the Otsu method and mask refinement as was done with the TFM. Point source detection was then done to identify the adhesions following by tracking the adhesions across time using Brownian and directed motion models. Focal adhesions were then segmented, analyzed, and then adhesions are classified by type.

4 Results

4.1 Rheology

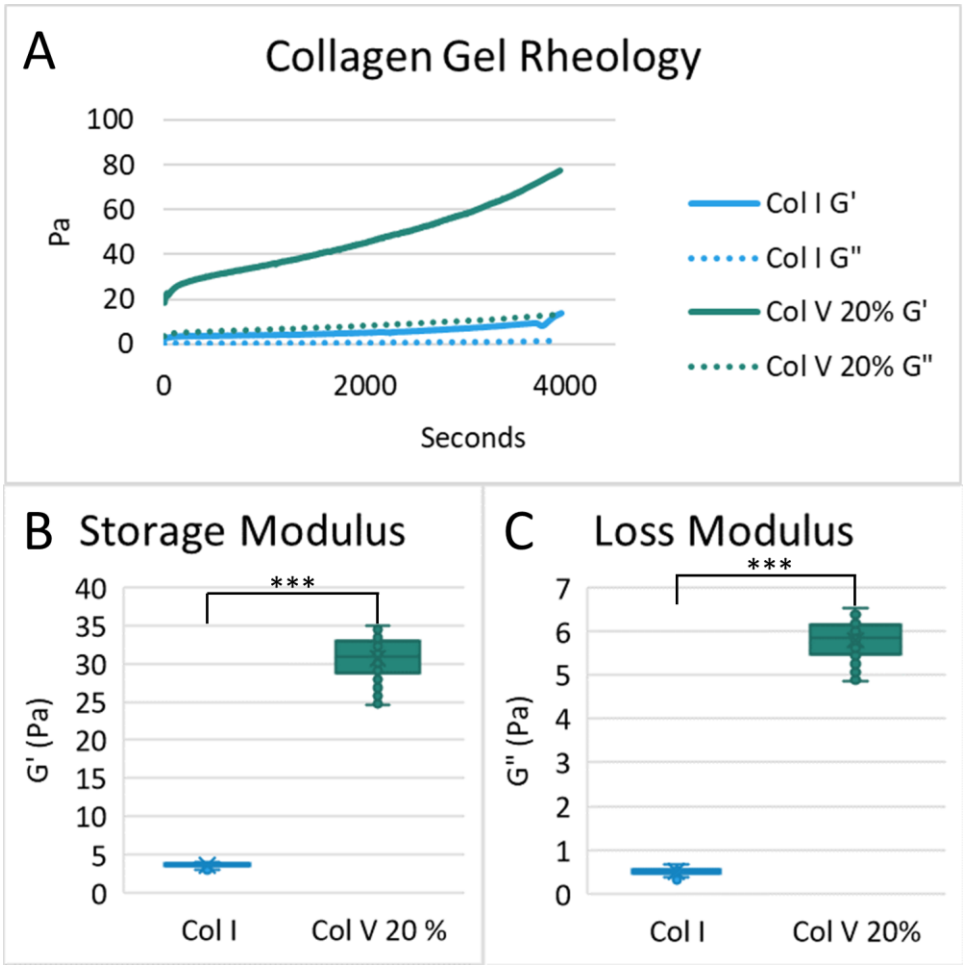

Figure 4.1 A) The storage and loss moduli at later time points are unreliable due to the gel drying out. B) The storage modulus is much greater for 20% collagen V. C) The loss modulus is much greater for 20% collagen V.

Initially, after curing, collagen gel made with 20% collagen V was stiffer. However, over the course of the experiment, there were problems with the gel drying out. This makes the data at later time points unreliable. Because of this, for statistical analysis, only time points between 100 and 1000 seconds were used. The storage modulus was greater for 20% collagen V (3.594 Pa collagen I, and 31.01 Pa 20 % collagen V). The loss modulus was also greater for collagen 20% V (0.5233 Pa collagen I, and 5.849 Pa 20% collagen V).

4.2 SEM

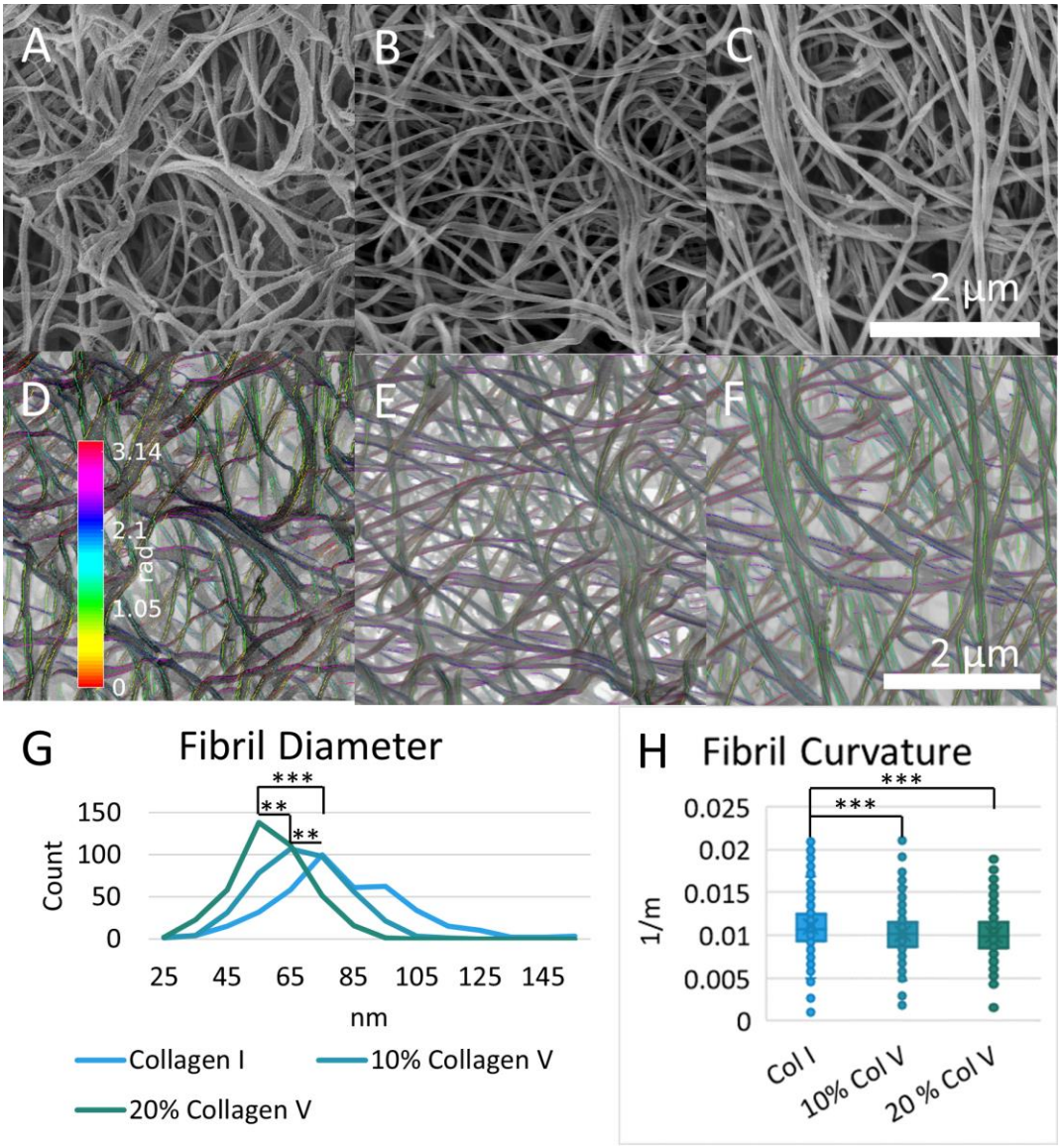

Figure 4.2 Representative images of A) Collagen I B) 10% collagen V C)20% collagen V. D-F) Segmentation of representative images. The angle of the fibril in radians is shown by its color. G) The diameter increases in both size variability with decreasing collagen V concentration H) The addition of collagen V reduces fibril curvature.

Collagen fibril diameter was greatest with 100% collagen I (78.9 nm), followed by 10% collagen V (67.61 nm), and 20% collagen V (57.93 nm). Variance of fibril diameter was decreased with increasing amounts of collagen V. Fibril curvature was reduced for collagen 10% collagen V (0.001682 1/m) and 20% collagen V (0.001727 1/m) compared to collagen I (0.001879 1/m).

4.3 TFM and Adhesion

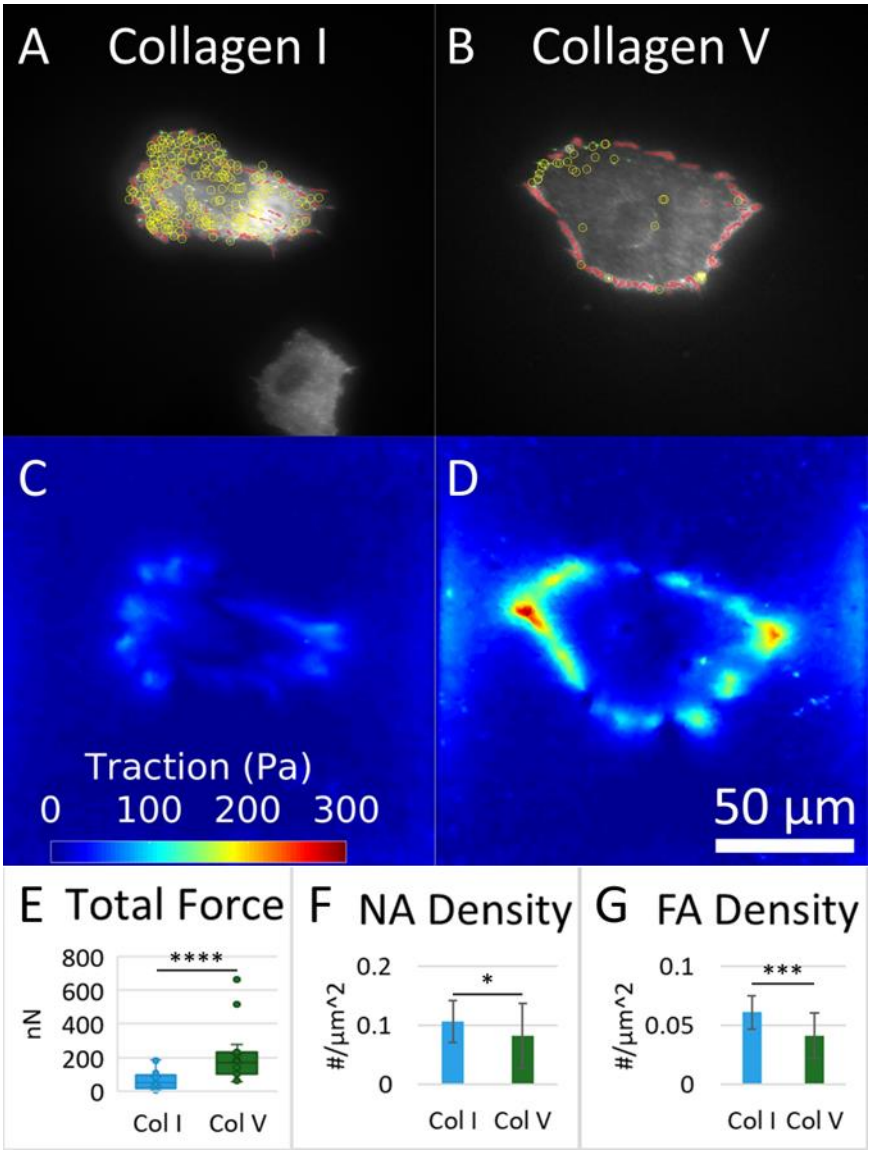

Figure 4.3 Preliminary TFM and adhesion data taken 4 hours after seeding A-B) Representative adhesion images. Yellow=nascent adhesions, green= focal complexes red=focal adhesions C-D) Representative traction maps E) Total force is increased on collagen V. F) Nascent adhesion density is reduced on collagen V G) Focal adhesion density is reduced on collagen V

Preliminary TFM data of cells cultured on telo collagen I and atelo collagen V imaged at 4 hours after seeding showed significant increases in average traction per cell. However, this was only intermittently replicated in later experiments. Once care was taken to ensure that all experiments were carried out on the same batch of TFM substrates the findings were replicated. For the final data, cells were seeded on atelo and telo collagen I and atelo collagen V and imaged 5 hours after seeding. Average traction per

cell was not statically different between atelo (35.8 Pa) and telo (48.4 Pa) collagen I but was increased on collagen V (89.9 Pa).

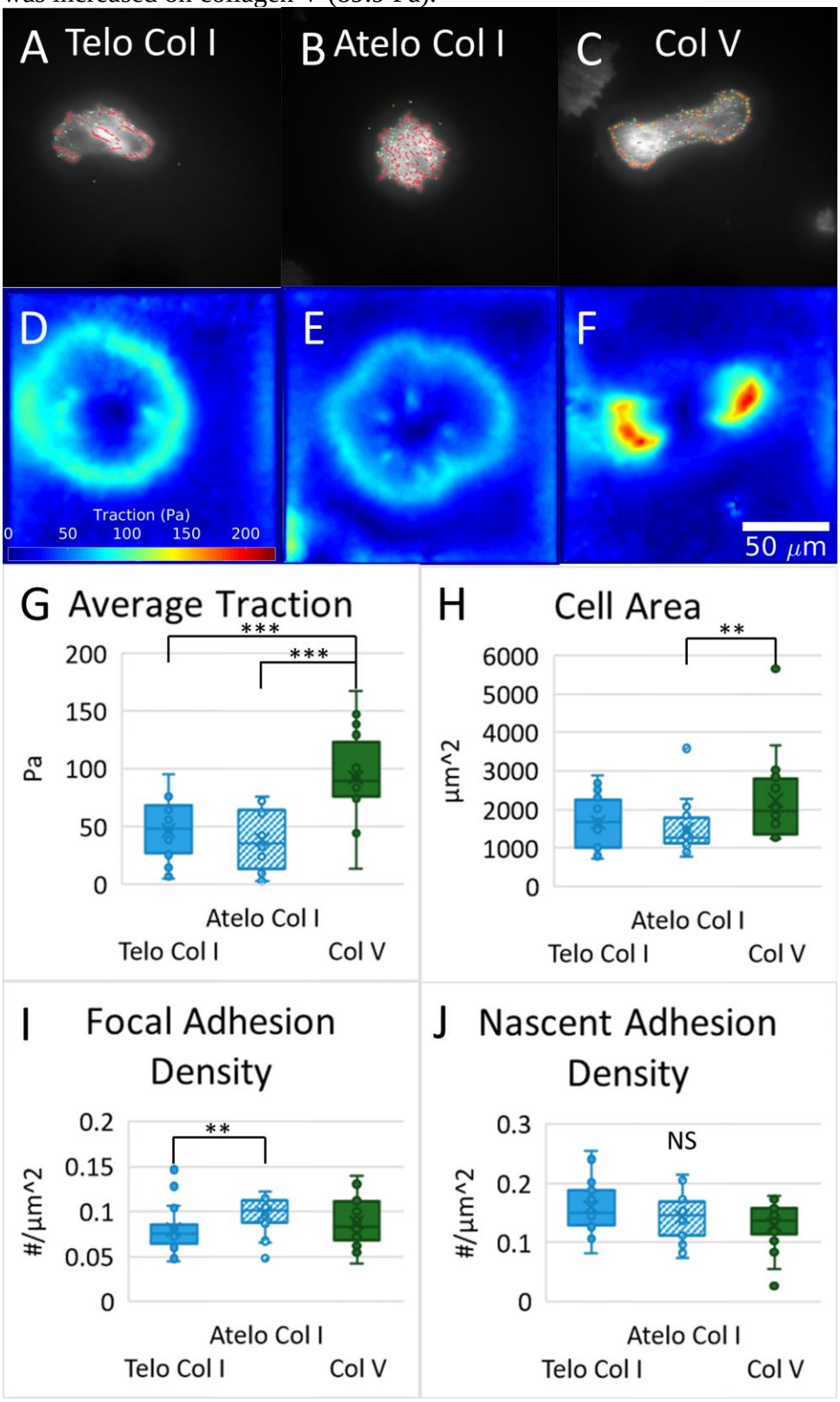

Figure 4.4 A-C) Representative adhesion images on telo collagen I, atelo collagen I and collagen V. Yellow=nascent adhesions, green= focal complexes red=focal adhesions. D-F) Representative traction maps. G) Average traction is increased on collagen V. H) Cell area is increased on collagen V I-J) Focal adhesion density and nascent and adhesion density are not statistically different on collagen V.

Preliminary adhesion data for adhesions on collagen V showed significantly lower adhesion density in both focal and nascent adhesions and disappearance of adhesions from the interior of the cells. Later experiments done 5 hours after seeding on telo and atelo collagen I and V failed to show a statically significant difference in adhesion density between cells cultured on collagen types I and V (0.07543 focal adhesions per μm^2 telo collagen I, 0.1019 focal adhesions per μm^2 atelo collagen I, 0.08278 focal adhesions per μm^2 collagen V, 0.1501 nascent adhesions per μm^2 telo collagen I, 0.1456 nascent adhesions per μm^2 atelo collagen I, and 0.1366 nascent adhesions per μm^2 collagen V). The disappearance of adhesions on the interior of cells cultured on collagen V was only intermittently observed in later experiments. Focal adhesion area was decreased on collagen V (0.5085 μm^2 telo collagen I, 0.4623 μm^2 atelo collagen I, and 0.4160 μm^2 collagen V). However, average traction force was still increased on collagen V (48.40 Pa telo collagen I, 35.79 Pa atelo collagen I, and 89.86 Pa collagen V) and spread area was increased on collagen V (1678 μm^2 telo collagen I, 1278 μm^2 atelo collagen I, and 1973 μm^2 collagen V).

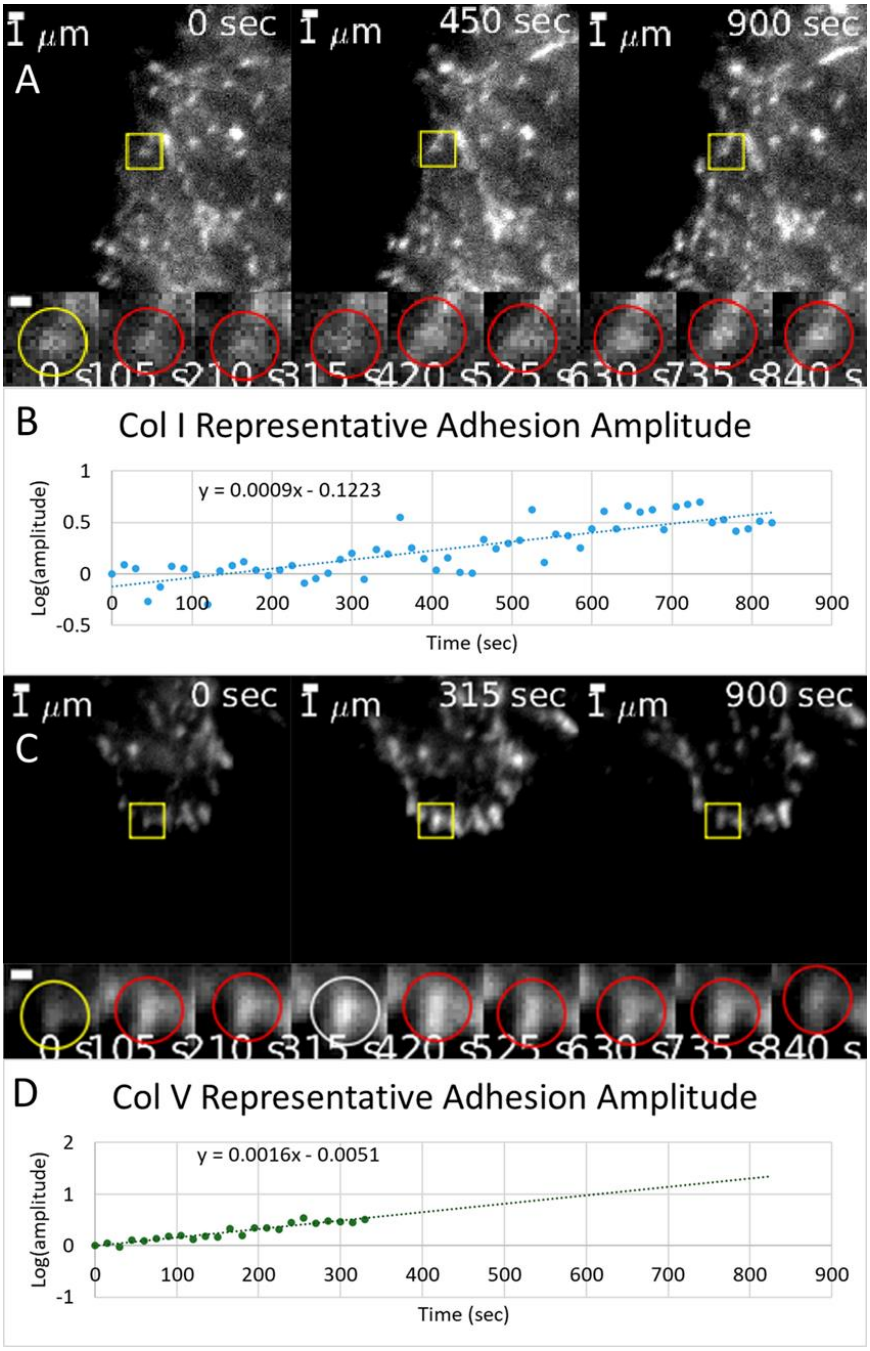

Figure 4.5 A-B) Representative adhesion assembly on collagen I. C-D) Representative adhesion assembly on collagen V. Adhesion assembly is more rapid on collagen V compared to collagen I.

For adhesion dynamics at 1.5 hours after seeding adhesion assembly rates were increased on collagen V. On average focal adhesion lifetime, was lower on collagen V (30 min collagen I vs 26 min collagen V), but longer among the subset of longer-lived adhesions (20 min collagen I vs 22.9 min collagen V). Both stable adhesion ratio (0.152

collagen I vs 0.191collagen V) and nucleating adhesion ratio (0.0336 collagen I vs 0.0423 collagen V) were higher on collagen V.

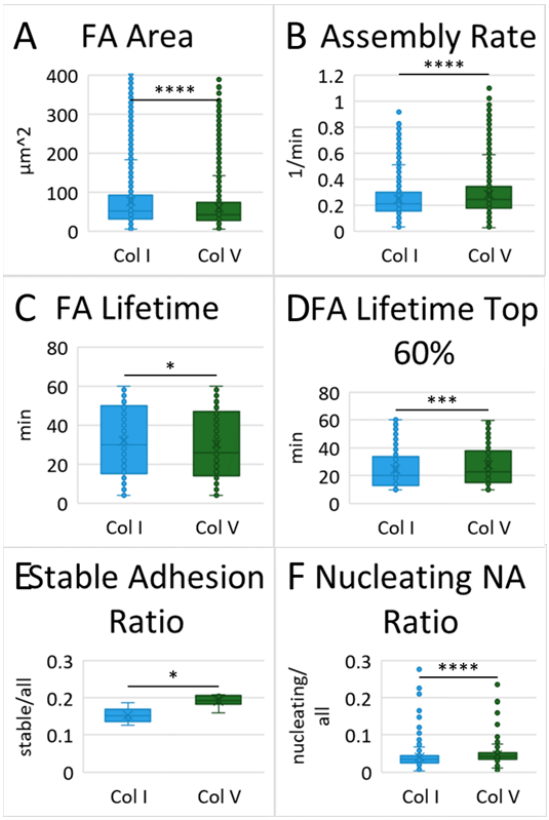

Figure 4.6 A) Focal adhesion area is increased on collagen I. B) Assembly rate is increased on collagen V. C) Focal adhesion lifetime among all focal adhesions is increased on collagen I D) Focal adhesion lifetime among longer lived adhesions is increased on collagen V. E) Stable adhesion ratio is increased on collagen V. F) Nucleating adhesion ratio is increased on collagen V.

5 Discussion

The findings that fibril diameter decreased with increasing collagen V content were expected because previous studies using precipitated fibrils had similar findings. Likewise, the finding that the addition of collagen V reduced the variability of fibril diameter is expected based on the observed distribution of precipitated fibrils and because large irregularly shaped collagen fibrils are found in the skin in cEDS [5, 40].

The decreased fibril curvature with the addition of collagen V implies that the fibrils themselves are stiffer. This would explain the 20% collagen V gel having a larger storage modulus. The fibril curvature in the gel being less implies that they have a greater persistence length. Persistence length is a function of bending stiffness (1). P is persistence length, B is bending stiffness, k_b is Boltzmann constant, and T is temperature. Because the temperature was the same for all conditions, only the bending stiffness could be what has changed.

(1) $P = \frac{B}{k_b T}$

Bending stiffness is a function of the second moment of area and Young's modulus (2). E is Young's modulus, and I is second moment of area. The second moment of area for a beam with a circular cross section is a function of radius (3).

(2) $B = EI$
(3) $I = \frac{\pi}{4} r^4$

Radius decreases with increasing collagen V content; this means that the second moment of area greatly decreases with increasing collagen V content. In order for bending stiffness to increase while the second moment of area is decreased the Young's modulus must be greatly increased [41].

In normal wound healing, myofibroblasts compact connective tissue and pulling together the edges of a wound [42]. In cEDS, wounds tend to heal with widened scarring. A failure of the fibroblasts to contract sufficiently to pull together the edges of the wound would explain this phenomenon [1].

The effects of collagen V on adhesion dynamics are complex. In cell migration, adhesions form at the leading edge of the cell. The increased rate of adhesion formation may be indicative of faster migration [43].

6 Conclusion

Collagen V increases fibroblast contractility and promotes adhesion nucleation. It is highly likely that this is due to nanoscale mechanical properties because bulk mechanical properties were controlled for in the experiment and there are not integrins specific to collagen V and not I. The increased nucleation of adhesions is suggestive of collagen V promoting migration, but this is complicated by there being a subset of adhesions that are longer lived on collagen V. Further experiments are necessary to determine the role of collagen V on fibroblast migration.

The increased storage modulus of a collagen gel containing 20% collagen V along with the decreased fibril curvature in gels containing collagen V is highly suggestive of collagen V increasing fibril bending stiffness. Experiments to directly measure fibril stiffness are currently being worked on.

7 Reference List

1. Bowen, J.M., et al. *Ehlers–Danlos syndrome, classical type*. in *American Journal of Medical Genetics Part C: Seminars in Medical Genetics*. 2017. Wiley Online Library.
2. Baeza-Velasco, C., R. Grahame, and J.F. Bravo, *A connective tissue disorder may underlie ESSENCE problems in childhood.* Research in Developmental Disabilities, 2017. **60**: p. 232-242.
3. Malfait, F., et al. *The 2017 international classification of the Ehlers–Danlos syndromes*. in *American Journal of Medical Genetics Part C: Seminars in Medical Genetics*. 2017. Wiley Online Library.
4. Royce, P., et al., *Brittle cornea syndrome: an heritable connective tissue disorder distinct from Ehlers-Danlos syndrome type VI and fragilitas oculi, with spontaneous perforations of the eye, blue sclerae, red hair, and normal collagen lysyl hydroxylation.* European journal of pediatrics, 1990. **149**(7): p. 465-469.
5. Hausser, I. and I. Anton-Lamprecht, *Differential ultrastructural aberrations of collagen fibrils in Ehlers-Danlos syndrome types I–IV as a means of diagnostics and classification.* Human genetics, 1994. **93**(4): p. 394-407.
6. Burch, G.H., et al., *Tenascin–X deficiency is associated with Ehlers–Danlos syndrome.* Nature genetics, 1997. **17**(1): p. 104-108.
7. Colige, A., et al., *Novel types of mutation responsible for the dermatosparactic type of Ehlers–Danlos syndrome (Type VIIC) and common polymorphisms in the ADAMTS2 gene.* Journal of Investigative Dermatology, 2004. **123**(4): p. 656-663.
8. Malfait, F., et al., *Three arginine to cysteine substitutions in the pro-alpha (I)-collagen chain cause Ehlers-Danlos syndrome with a propensity to arterial rupture in early adulthood.* Human mutation, 2007. **28**(4): p. 387-395.
9. Fukada, T., et al., *The zinc transporter SLC39A13/ZIP13 is required for connective tissue development; its involvement in BMP/TGF-β signaling pathways.* PloS one, 2008. **3**(11): p. e3642.
10. Rohrbach, M., et al., *Phenotypic variability of the kyphoscoliotic type of Ehlers-Danlos syndrome (EDS VIA): clinical, molecular and biochemical delineation.* Orphanet journal of rare diseases, 2011. **6**(1): p. 1-9.
11. Hermanns-Lê, T., et al., *Dermal ultrastructure in low Beighton score members of 17 families with hypermobile-type Ehlers-Danlos syndrome.* Journal of Biomedicine and Biotechnology, 2012. **2012**.
12. Kapferer-Seebacher, I., et al., *Periodontal Ehlers-Danlos syndrome is caused by mutations in C1R and C1S, which encode subcomponents C1r and C1s of complement.* The American Journal of Human Genetics, 2016. **99**(5): p. 1005-1014.
13. Blackburn, P.R., et al., *Bi-allelic alterations in AEBP1 lead to defective collagen assembly and connective tissue structure resulting in a variant of Ehlers-Danlos syndrome.* The American Journal of Human Genetics, 2018. **102**(4): p. 696-705.

14. Van Damme, T., et al., *Biallelic B3GALT6 mutations cause spondylodysplastic Ehlers–Danlos syndrome.* Human molecular genetics, 2018. **27**(20): p. 3475-3487.
15. Ayoub, S., et al., *Clinical features, molecular results, and management of 12 individuals with the rare arthrochalasia Ehlers-Danlos syndrome.* American Journal of Medical Genetics Part A, 2020. **182**(5): p. 994-1007.
16. Delbaere, S., et al., *Novel defects in collagen XII and VI expand the mixed myopathy/Ehlers–Danlos syndrome spectrum and lead to variant-specific alterations in the extracellular matrix.* Genetics in Medicine, 2020. **22**(1): p. 112-123.
17. Kosho, T., et al., *Recent advances in the pathophysiology of musculocontractural Ehlers-Danlos syndrome.* Genes, 2020. **11**(1): p. 43.
18. Malek, S. and D.V. Köster, *The Role of Cell Adhesion and Cytoskeleton Dynamics in the Pathogenesis of the Ehlers-Danlos Syndromes and Hypermobility Spectrum Disorders.* Frontiers in Cell and Developmental Biology, 2021. **9**: p. 883.
19. Kobayasi, T., *Abnormality of dermal collagen fibrils in Ehlers Danlos syndrome. Anticipation of the abnormality for the inherited hypermobile disorders.* European Journal of Dermatology, 2004. **14**(4): p. 221-229.
20. Proske, S., et al., *Ehlers-Danlos syndrome–20 years experience with diagnosis and classification.* JDDG: Journal der Deutschen Dermatologischen Gesellschaft, 2006. **4**(4): p. 308-318.
21. Angwin, C., et al., *Absence of collagen flowers on electron microscopy and identification of (Likely) pathogenic COL5A1 variants in two patients.* Genes, 2019. **10**(10): p. 762.
22. Viglio, S., et al., *Rescue of migratory defects of Ehlers–Danlos syndrome fibroblasts in vitro by type V collagen but not insulin-like binding protein-1.* Journal of investigative dermatology, 2008. **128**(8): p. 1915-1919.
23. Zoppi, N., et al., *Dermal fibroblast-to-myofibroblast transition sustained by αvβ3 integrin-ILK-Snail1/Slug signaling is a common feature for hypermobile Ehlers-Danlos syndrome and hypermobility spectrum disorders.* Biochimica et Biophysica Acta (BBA)-Molecular Basis of Disease, 2018. **1864**(4): p. 1010-1023.
24. Shoulders, M.D. and R.T. Raines, *Collagen structure and stability.* Annual review of biochemistry, 2009. **78**: p. 929-958.
25. Mak, K.M., C.Y.M. Png, and D.J. Lee, *Type V collagen in health, disease, and fibrosis.* The Anatomical Record, 2016. **299**(5): p. 613-629.
26. Miklovic, T. and V.C. Sieg, *Ehlers danlos syndrome.* 2019.
27. Catala-Pétavy, C., et al., *Contribution of skin biometrology to the diagnosis of the Ehlers–Danlos syndrome in a prospective series of 41 patients.* Skin Research and Technology, 2009. **15**(4): p. 412-417.
28. Brady, A.F., et al. *The Ehlers–Danlos syndromes, rare types*. in *American Journal of Medical Genetics Part C: Seminars in Medical Genetics*. 2017. Wiley Online Library.

29. Mao, J.-R. and J. Bristow, *The Ehlers-Danlos syndrome: on beyond collagens.* The Journal of clinical investigation, 2001. **107**(9): p. 1063-1069.
30. Zoppi, N., et al., *Human fibroblasts with mutations in COL5A1 and COL3A1 genes do not organize collagens and fibronectin in the extracellular matrix, down-regulate α2β1 integrin, and recruit αvβ3 instead of α5β1 integrin.* Journal of Biological Chemistry, 2004. **279**(18): p. 18157-18168.
31. Berendsen, A.D., et al., *Collagen type V enhances matrix contraction by human periodontal ligament fibroblasts seeded in three-dimensional collagen gels.* Matrix biology, 2006. **25**(8): p. 515-522.
32. Zeltz, C., J. Orgel, and D. Gullberg, *Molecular composition and function of integrin-based collagen glues—introducing COLINBRIs.* Biochimica et Biophysica Acta (BBA)-General Subjects, 2014. **1840**(8): p. 2533-2548.
33. *Bovine Type V Collagen Solution*. [cited 2023; Available from: https://www.southernbiotech.com/bovine-type-v-collagen-solution-1280-02s.
34. *Telo Collagen vs Atelo Collagen Amino Acid Sequence*. [cited 2023; Available from: https://advancedbiomatrix.com/telocollagen-vs-atelocollagen-amino-acid-sequence.html#:~:text=Telocollagen%20(acid%20extracted)%20and%20Atelocollagen,will%20also%20be%20much%20stronger.
35. Gutierrez, E., et al., *High refractive index silicone gels for simultaneous total internal reflection fluorescence and traction force microscopy of adherent cells.* PLoS One, 2011. **6**(9): p. e23807.
36. Suñé-Auñón, A., et al., *Full L1-regularized traction force microscopy over whole cells.* BMC bioinformatics, 2017. **18**(1): p. 1-14.
37. *QGel 920 Silicone Encapsulants*. [cited 2023; Available from: https://cht-silicones.com/products/encapsulants/QGel%20920.
38. Lanni, F., A.S. Waggoner, and D.L. Taylor, *Structural organization of interphase 3T3 fibroblasts studied by total internal reflection fluorescence microscopy.* The Journal of cell biology, 1985. **100**(4): p. 1091-1102.
39. Michel, R., et al., *Inverse problems for the determination of traction forces by cells on a substrate: a comparison of two methods.* Computer Methods in Biomechanics and Biomedical Engineering, 2012. **15**(sup1): p. 27-29.
40. Linsenmayer, T.F., et al., *Type V collagen: molecular structure and fibrillar organization of the chicken alpha 1 (V) NH2-terminal domain, a putative regulator of corneal fibrillogenesis.* The Journal of cell biology, 1993. **121**(5): p. 1181-1189.
41. Manning, G.S., *The persistence length of DNA is reached from the persistence length of its null isomer through an internal electrostatic stretching force.* Biophysical journal, 2006. **91**(10): p. 3607-3616.
42. Chitturi, R.T., et al., *The role of myofibroblasts in wound healing, contraction and its clinical implications in cleft palate repair.* Journal of international oral health: JIOH, 2015. **7**(3): p. 75.
43. Huttenlocher, A., R.R. Sandborg, and A.F. Horwitz, *Adhesion in cell migration.* Current opinion in cell biology, 1995. **7**(5): p. 697-706.

A Copyright documentation

All images are used under fair use.

Figure 1.2 Mao, J.-R. and J. Bristow, *The Ehlers-Danlos syndrome: on beyond collagens.* The Journal of clinical investigation, 2001. **107**(9): p. 1063-1069.

Figure 1.3 Baeza-Velasco, C., R. Grahame, and J.F. Bravo, *A connective tissue disorder may underlie ESSENCE problems in childhood.* Research in Developmental Disabilities, 2017. **60**: p. 232-242.
Malfait, F., et al. *The 2017 international classification of the Ehlers–Danlos syndromes*. in *American Journal of Medical Genetics Part C: Seminars in Medical Genetics*. 2017. Wiley Online Library.

Figure 1.4 Zoppi, N., et al., *Human fibroblasts with mutations in COL5A1 and COL3A1 genes do not organize collagens and fibronectin in the extracellular matrix, down-regulate α2β1 integrin, and recruit αvβ3 instead of α5β1 integrin.* Journal of Biological Chemistry, 2004. **279**(18): p. 18157-18168.
Viglio, S., et al., *Rescue of migratory defects of Ehlers–Danlos syndrome fibroblasts in vitro by type V collagen but not insulin-like binding protein-1*. Journal of investigative dermatology, 2008. **128**(8): p. 1915-1919.

Figure 3.2 Suñé-Auñón, A., et al., *Full L1-regularized traction force microscopy over whole cells.* BMC bioinformatics, 2017. **18**(1): p. 1-14.